

XR Capacity Enhancement through Multi-Connected XR Tethering Groups

Muhammad Ahsen , Graduate Student Member, IEEE, Boyan Yanakiev, Claudio Rosa, and Ramoni Adeogun , Senior Member, IEEE

Abstract—Extended Reality (XR) applications have limited capacity in 5th generation-advanced (5G-A) cellular networks due to high throughput requirements coupled with strict latency and high reliability constraints. To enhance XR capacity in the downlink (DL), this paper investigates multi-connected XR tethering groups (TGrs), comprising an XR device and a cooperating 5G-A device. This paper presents investigations for two types of cooperation within XR TGr, i.e., selection combining (SC) and soft combining and their impact on the XR capacity of the network. These investigations consider joint hybrid automatic repeat request (HARQ) feedback processing algorithm and also propose enhanced joint Outer Loop Link Adaptation (OLLA) algorithm to leverage the benefits of multi-connectivity. These enhancements aim to improve the spectral efficiency of the network by limiting HARQ retransmissions and enabling the use of higher modulation and coding scheme (MCS) indices for given signal-to-interference-plus-noise ratio (SINR), all while maintaining or operating below than the target block error rate (BLER). Dynamic system-level simulation demonstrate that XR TGrs with soft combining achieve performance improvements of 23 - 42% in XR capacity with only XR users and 38-173% in the coexistence scenarios consisting of XR users and enhanced mobile broadband (eMBB) user. Furthermore, the enhanced joint OLLA algorithm enables similar performance gains even when only one device per XR TGr provides channel state information (CSI) reports, compared to scenarios where both devices report CSI. Notably, XR TGrs with soft combining also enhance eMBB throughput in coexistence scenarios.

Index Terms—XR, Wireless tethering, Cooperative Communication, MBS, HARQ, tethering group.

I. Introduction

Extended Reality (XR) has applications across a wide range of domains including education, healthcare, gaming and autonomous driving etc. It is recognized as one of the key use cases for future wireless networks [1]. XR services typically impose stringent quality of service (QoS) requirements, with latency constraints ranging from 5 to 15 milliseconds and data rate demands between 30 and 60 Mbps [2]. Additionally, high reliability typically at 99% level is essential.

Several studies have investigated the feasibility of 5th generation-advanced (5G-A) cellular networks for supporting XR applications [3]–[6]. However, due to the strict

Muhammad Ahsen and Ramoni Adeogun are with the Department of Electronic Systems, Technical Faculty of IT and Design, Aalborg University, 9220 Aalborg, Denmark (e-mail: muah@es.aau.dk; ra@es.aau.dk).

Boyan Yanakiev and Claudio Rosa are with the Nokia, DK-9220 Aalborg, Denmark (e-mail: boyan.yanakiev@nokia.com; claudio.rosa@nokia.com)

QoS requirements, the number of XR users that 5G-A can support remains limited. This limitation underscores the need for more efficient wireless network solutions capable of delivering seamless XR experience at scale.

Among various techniques under investigation, multi-connectivity has emerged as one of the promising approach for enhancing XR performance [7]–[10]. Research on millimeter-wave networks [7] and [8] has shown that multi-connectivity can improve user density and mitigate the effects of blockages, thereby enhancing the XR user experience. In [9], a dual connectivity architecture leveraging both sub-6 GHz and millimeter-wave frequencies, combined with mobile edge capability, was proposed to improve virtual reality (VR) reliability. Further, [10] examined XR capacity improvements in coexistence scenarios involving XR and broadband traffic by employing multi-connectivity across sub-6 GHz and millimeter-wave bands. Despite these advantages, traditional multi-connectivity approaches, which rely on multiple point-to-point (PTP) connections, consume significant radio resources. Similar approaches have been studied for Ultra Reliable Low Latency Communications (URLLC) applications in the sub-6 GHz band. Although these approaches improve transmission reliability, they degrade spectral efficiency and overall network throughput [11], [12]. Thus direct application of such PTP-based multi-connectivity methods to XR over sub-6 GHz frequencies is impractical, as it further constrains XR capacity.

To address this, we explore XR tethering groups (TGrs) as a means of utilizing multi-connectivity benefits without the associated cellular network resource overhead. XR tethering group (TGr)s enable multiple connections (direct and indirect) for an XR device via point-to-multipoint (PTM) transmissions [13]–[15]. Each TGr consists of an XR device and a 5G-A device with tethering capability referred to as the tethering device, which are also interconnected via a tethering link [16]. Within a TGr, the tethering device forwards received data to the XR device, creating cooperative communication between the two devices.

We investigate two cooperation schemes for TGrs under PTM transmission from the cellular network, i.e., selection combining (SC) and soft combining. In SC, the XR device can select the transport block (TB) from either the direct link or the indirect link. In soft combining, the XR device performs soft-bit level combining of TBs received from both links. This is analogous to hybrid automatic

repeat request (HARQ) with Chase combining (CC) where soft bits from repeated transmissions are combined to improve decoding performance [17] [18]. In case of HARQ retransmission with CC, cellular network's radio resources are doubled for sending the same TB assuming the HARQ retransmission is scheduled with same modulation and coding scheme (MCS). However, in XR TGr, XR device has two copies of the same TB (or two sets of the soft bits corresponding to the same TB) which traversed through different channel conditions while utilizing single cellular network resources (assuming tethering link operate on different carrier frequency).

Prior work [13] and [14] has proposed joint HARQ feedback processing algorithm for PTM transmission towards the XR TGr to enhance the spectrum efficiency by incorporating the cooperation benefits in HARQ retransmission from the network. However, these studies assumed a static MCS and did not consider dynamic Link Adaptation (LA) with investigations limited to link-level. In [15], we extended this investigation by evaluating XR TGrs using SC with dynamic LA in system-level simulations. This paper further advances our work by considering soft combining with dynamic LA for XR TGrs in system-level evaluations and its impact on XR capacity. Our focus is to assess how XR TGrs employing selection/soft combining affect overall XR capacity of the network under PTM transmission.

LA is employed to select the optimal MCS based on channel quality indicator (CQI) indicator provided in the channel state information (CSI) report by the User Equipment (UE) [19]. To address imperfections in CQI indicator, stemming from quantization errors, measurement inaccuracies, feedback delays and temporal channel fluctuations, Outer Loop Link Adaptation (OLLA) is applied. OLLA dynamically adjusts the MCS selection using HARQ feedback to maintain a predefined target block error rate (BLER) [20], thereby improving the robustness and reliability of the LA mechanism.

The investigations in [15] concludes that traditional OLLA, which relies solely on HARQ feedback from a single UE (i.e., OLLA fixed to one UE) is insufficient to translate TGr cooperative gains into LA improvements. Instead, a joint OLLA is required to leverage these cooperative benefits in LA. However, the joint OLLA algorithm proposed in [15] for PTM transmission with cooperating users is limited to SC use cases only. In this paper, we are extending our previous work of [15], by proposing an enhanced joint OLLA algorithm for PTM transmission with cooperating users that supports both SC and soft combining. The goal is to exploit device cooperation within the TGr to enable higher MCS selection, reducing latency and improving spectral efficiency. This can increase the number of XR users meeting QoS requirements and/or free up resources for other services.

Coexistence scenarios, i.e., XR users with enhanced mobile broadband (eMBB) users have also been examined in available literature related to XR [21], [22], which showed that eMBB users negatively impact XR capacity

due to inter-cell interference (ICI). However, these studies considered only single-link-connected XR users. Here, we investigate XR TGrs in the presence of eMBB users to assess their impact on XR performance or capacity and potential improvements in eMBB throughput, given the lower resource consumption of XR TGrs.

Additionally, we extend the limited code block (CB) based soft combining initially proposed in [14], which was confined to a single TGr and static LA. Our current investigation evaluates CB-based soft combining in a multi-cell network with multiple XR TGrs and dynamic LA, measuring its impact on XR capacity. In this approach, the XR device treats CBs received from the tethering device similar to code block group (CBG) based HARQ retransmissions [3] but without consuming additional radio resources (assuming tethering link operates on a separate carrier).

Our major contributions are summarized as follows

- We investigate the XR capacity of the network with XR TGrs with Selection/Soft Combining Scheme (SSCS) under PTM transmission, employing joint HARQ and LA in a system-level simulation calibrated according to [2] for Dense Urban (DU) and Indoor Hotspot (InH) scenarios, each with unique channel conditions, cell deployments and user densities [23].
- We propose an enhanced joint OLLA algorithm for PTM transmission that supports both SC and SSCS, leveraging cooperation to enable higher MCS selection.
- We analyze the performance of XR TGrs with SSCS in the presence of eMBB user, evaluating both the impact on XR TGr performance and the potential throughput gains for eMBB.
- We investigate XR capacity enhancements through limited CB-based cooperation within a TGr using SSCS.

The structure of the article is as follows: Section II outlines the system model followed by the cooperation and adaptation techniques for XR TGr in Section III and CB-based cooperation in Section IV. Section V details the evaluation methodology. Simulation results are discussed in Section VI and the conclusion is presented in VII.

II. System Model

This study considers a multi-cell downlink (DL) network comprising multiple XR TGrs. Each TGr consists of an XR UE (UE-X) and a tethering UE (UE-T). Both UEs in a TGr are connected to the same Next-Generation Node B (gNodeB) and are members of the same 5G-A multicast session [24]. However, each TGr is associated with a distinct multicast session to avoid inter-group overlap. The location of TGrs within a cell is random. Within a TGr, UE-T is positioned at a fixed distance x from UE-X. Each 5G-A multicast session delivers identical data to both UEs in a TGr using PTM transmission, applicable to both initial transmissions and any HARQ retransmissions. In the remainder of the paper, a multicast session with

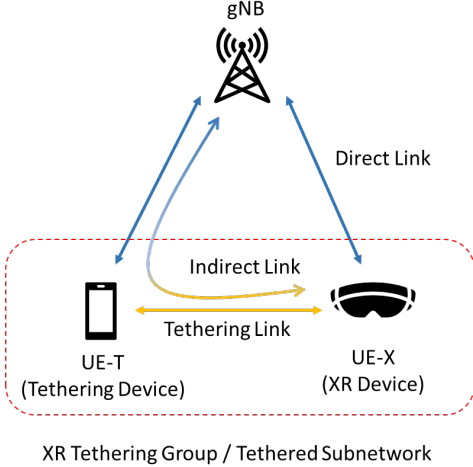


Fig. 1: XR TGr.

cooperating member UEs is referred to as a cooperative multicast session. Within a TGr, UE-T assists UE-X by relaying XR data over a tethering link [16], effectively providing UE-X with an additional indirect link from the gNodeB (via UE-T), as shown in Figure 1.

Asynchronous HARQ is modeled, where each UE within a TGr independently provides HARQ feedback based on its initial decoding of the TB [28]. We consider both Inner Loop Link Adaptation (ILLA) and OLLA for PTM transmissions configured for XR TGrs. While ILLA governs the selection of MCS based on CSI, OLLA adjust MCS to achieve the target BLER.

The tethering link is assumed to operate on a carrier frequency that is different from the one used by the cellular network. It may utilize either wireless local-area network (WLAN) or 5th generation (5G) sidelink technologies [16]. While the performance of the tethering link impacts the overall performance of the TGr, this study focuses on assessing the upper-bound capacity gains achievable through multi-connected TGrs. In line with the objective, the tethering link is modeled with the following assumptions:

- For the direct link (UE-gNodeB) and the tethered link (UE-X to UE-T), we assume the usage of distinct radio interfaces running on distinct carrier frequencies to enable simultaneous communication with no notable in-device-coexistence issues.
- The tethering link is additionally assumed to have enough capacity to handle the data load, ideal channel conditions and zero processing/decoding and forwarding delays.

III. Cooperation and Adaptation Techniques for XR TGr

A. Cooperation in XR TGr

We consider following two cooperation schemes for TGr.

- Selection Combining Scheme (SCS): In this scheme, UE-T decodes the received TB and forwards it to

UE-X using the tethering link, following decode-and-forward (DF) algorithm [25]. UE-X performs SC over the two TB copies, one from the direct gNodeB-UE-X link and one from the indirect gNodeB-UE-T-UE-X link. If UE-X successfully decodes the TB via the direct link, it discards the TB if received from UE-T. If decoding fails at UE-X, then it uses the TB if received from UE-T via a tethering link.

- SSCS: This scheme extends SCS by introducing soft combining, depending on decoding outcomes at both UEs of the TGr. If UE-T successfully decodes the TB, it forwards the decoded TB to UE-X using the DF algorithm. If UE-T fails to decode the physical downlink shared channel (PDSCH) but successfully decodes the physical downlink control channel (PDCCH), it forwards soft values corresponding to that TB using a soft decode-and-forward (soft-DF) approach [26]. UE-X then applies either SC or soft combining, based on its own decoding outcome of PDSCH and PDCCH. The purpose of SSCS is to reduce the data overhead on the tethering link and/or minimize the computational burden on UE-X, by switching intelligently between SC and soft combining. The details regarding the overhead impact of different cooperation scheme can be found in our prior work in [14]. In soft combining, UE-X adds the soft bits (log-likelihood ratio (LLR)) from the two sources, direct link and indirect link. The sign and magnitude of each LLR represents the bit decision and its confidence level, respectively [27].

The behavior of the TGr under different decoding scenarios of PDCCH and PDSCH assuming Rank-1 transmission is summarized in Table I. In the table, "D" indicates successful decoding, while "N/D" indicates decoding failure. TB_T and TB_X represent the decoded TBs at UE-T and UE-X, respectively. Similarly $softTB_T$ and $softTB_X$ represent soft bits of the TB at UE-T and UE-X respectively. From Table I, it can be seen that SCS offers gains in scenarios 2 and 3 only, whereas SSCS offers gains in scenario 5 as well if TB is decoded after soft combining, in addition to scenarios 2 and 3. To fully exploit the potential performance improvements offered by these cooperation schemes, modifications are required in both the HARQ retransmission logic and the LA algorithms at the network side. These updates are essential to adaptively select appropriate MCS values and retransmission policies based on decoding pattern after cooperation between the UEs of the TGr.

B. HARQ in XR TGr

For each TGr, a joint HARQ feedback processing algorithm proposed in [14] is implemented at the gNodeB. In case of SSCS, UE-X provides additional HARQ feedback only if it performs soft combining whereas in SCS, UE-X does not provide any additional HARQ feedback after performing SC. The joint HARQ feedback processing algorithm limits retransmission to only the following scenarios

TABLE I: PDCCH and PDSCH Decoding Status (Successfully Decoded: D and Fail to Decode: N/D) and Cooperation Strategies for the Tethering Group with SCS and SSCS

| Scenario | UE-T | | UE-X | | SCS | | SSCS | | | |
|----------|-------|-------|-------|-------|------------------|-------------------------|------------------|-----------------------------|--|--|
| | PDCCH | PDSCH | PDCCH | PDSCH | Relaying at UE-T | Combining at UE-X | Relaying at UE-T | Combining at UE-X | | |
| 1 | D | D | D | D | TBT | Discard TB _T | TBT | Discard TB _T | | |
| 2 | D | D | D | N/D | | | | Use TB _T | | |
| 3 | D | D | N/D | N/D | | Use TB _T | | Discard softTB _T | | |
| 4 | D | N/D | D | D | | | | | | |
| 5 | D | N/D | D | N/D | | | | | | |
| 6 | D | N/D | N/D | N/D | | softTB _T | | | | |
| 7 | N/D | N/D | D | D | | | | | | |
| 8 | N/D | N/D | D | N/D | | | | | | |
| 9 | N/D | N/D | N/D | N/D | | | | | | |

- For SCS: HARQ retransmission is triggered only if both UE-T and UE-X fail to decode the TB.
- For SSCS: HARQ retransmission is triggered only if UE-X fails to decode the TB even after soft combining the soft bits received from direct and indirect link.

This joint HARQ feedback processing algorithm increases spectral efficiency by reducing unnecessary retransmissions from the gNodeB, thereby exploiting the benefits of intra-TGr cooperation.

C. LA in XR TGr

1) ILLA in XR TGr: We study MCS selection under two CSI reporting configurations per XR TGr:

- CSI UE-X: Only UE-X provides periodic CSI reports. The gNodeB selects the MCS and precoding weights for the PTM transmission based solely on the CQI and channel estimates from UE-X.
- CSI Best: Both UE-T and UE-X per TGr provide periodic CSI reports. The gNodeB then selects the better of the two CSI reports (based on higher CQI) to determine the MCS and precoding weights for the PTM transmission towards that XR TGr.

2) OLLA in XR TGr: As per the existing LA algorithm, the gNodeB can select the MCS index η^* for a transmission as follows

$$\eta^* = \arg \max_{\eta} (R_{\eta} | \text{TBLER}_{\text{UE}} \leq \text{TBLER}^T) \quad (1)$$

where TBLER_{UE} is the perceived transport block error rate of the UE (could be UE-X or UE-T), TBLER^T is the target TBLER and R_{η} denotes the data rate associated with MCS index η . Practically, the UE determines its DL MCS by comparing its measured signal-to-interference-plus-noise ratio (SINR) with an internal lookup table mapping SINR values to TBLER for each MCS. This result is then reported to the gNodeB in CQI report. Notably, this step is carried out without considering cooperation, as done in conventional UE. The reported SINR is further adjusted to account for the inaccuracies in the CQI by an OLLA offset, based on HARQ feedback, which also does not reflect cooperation gains directly.

Therefore, for XR TGr we want to select the MCS index η^* based on the perceived post-cooperation TBLER of TGr, i.e., $\text{TBLER}_{\text{TGr}}$, as follows

$$\eta^* = \arg \max_{\eta} (R_{\eta} | \text{TBLER}_{\text{TGr}} \leq \text{TBLER}^T) \quad (2)$$

However, $\text{TBLER}_{\text{TGr}}$ is not directly available, as both UEs (UE-X and UE-T) provide HARQ feedback based on its initial decoding of the TB. In addition to the initial HARQ feedback, UE-X in SSCS cooperation scheme also provide 2nd HARQ feedback corresponding to the same TB after soft combining (when the initial decoding fails at both UE but is successful after combining soft bits at UE-X). To implement (2) and fully translate the cooperation benefits in LA, we propose an enhanced joint OLLA algorithm. This algorithm modifies the SINR used for MCS selection by incorporating the cooperation gain and handles multiple HARQ feedback corresponding to the same TB for SSCS. The enhanced joint OLLA algorithm for PTM multicast transmission to TGr is summarized in Algorithm 1. It first computes a joint HARQ feedback (HF_J) based on the individual HARQ feedbacks from UE-X and UE-T, which is then used for calculating the OLLA correction offset. An OLLA correction offset Δ_{OLLA} is applied to the SINR to compensate for CQI inaccuracies and include the benefits of cooperation. If γ^{TGr_i} is the reported SINR of TGr, i , the effective SINR, $\gamma_{eff}^{TGr_i}$, for MCS selection for PTM multicast transmission is calculated as

$$\gamma_{eff}^{TGr_i} = \gamma^{TGr_i} - \Delta_{\text{OLLA}}(i) \quad (3)$$

The offset $\Delta_{\text{OLLA}}(i)$ is initialized to a fixed value and is decreased by Δ_{down} when HF_J is positive acknowledgment (ACK) (promoting higher MCS selection) and increased by Δ_{up} when HF_J is negative acknowledgment (NACK) (promoting lower MCS selection). γ^{TGr_i} is determined by the configured CSI reporting scheme and can be calculated as

$$\gamma^{TGr_i} = \begin{cases} \max(\gamma^{UE-X_i}, \gamma^{UE-T_i}), & \text{if CSI Best} \\ \gamma^{UE-X_i}, & \text{if CSI UE-X} \end{cases} \quad (4)$$

where γ^{UE-X_i} and γ^{UE-T_i} is the SINR reported by UE-X and UE-T of TGr i in the CSI. The enhanced joint OLLA implements (2) for each TGr i as follows

$$\eta_i^* = \arg \max_{\eta_i} \left(R_{\eta_i} | 1 - P_{TGr_i}^{succ}(\gamma_{eff}^{TGr_i}, \eta_i) \leq \text{TBLER}^T \right) \quad (5)$$

where $P_{TGr_i}^{succ}(\gamma_{eff}^{TGr_i}, \eta_i)$ is the probability of success of TB decoding for TGr i after cooperation for MCS index η . This algorithm ensures that PTM multicast transmission to a TGr selects an MCS that is at least as high as that used for a unicast transmission to UE-X and typically higher when cooperation gains are present. In the absence of cooperation gains, the selected MCS matches that of the unicast case.

The proposed method extends the joint OLLA algorithm of [15], which supports only SC cooperation. Our enhanced version works with both SCS and SSCS, leveraging the additional second HARQ feedback in SSCS and incorporating soft combining gain into LA.

Algorithm 1 Enhanced JOINT OLLA

```

 $\{HF_{X1}, HF_{T1}\} \rightarrow 1^{\text{st}}$  HARQ feedback from {UE-X, UE-T}
 $HF_{X2} \rightarrow 2^{\text{nd}}$  HARQ feedback from UE-X
 $HF_J \rightarrow$  Joint HARQ feedback input to OLLA
 $CS \rightarrow$  Cooperation Scheme (SC, SSCS)
if  $CS = \text{SC}$  or ACK is received in  $1^{\text{st}}$  HARQ feedback then
   $HF_J = HF_{X1} \vee HF_{T1}$ 
  where  $\vee$  represents logical OR
else
   $HF_J = HF_{X2}$ 
end if

```

The operation of joint HARQ and enhanced joint OLLA for different decoding scenarios of PDCCH and PDSCH (assuming Rank-1 transmission for each PTM transmission to a TGr) is summarized in Table II. It can be seen that joint HARQ and enhanced joint OLLA effectively utilize cooperation based reliability gains to increase spectral efficiency of the network by choosing higher MCS values and avoiding redundant HARQ retransmissions. For SCS, HARQ retransmissions are avoided in scenarios 2 and 3, with OLLA step down (Δ_{down}) is applied in both cases. For SSCS, HARQ retransmissions are additionally avoided in scenario 5 when ACK is received after soft combining, with OLLA step down (Δ_{down}) is applied in scenarios 2, 3 and 5.

IV. CB based Cooperation

We extend our investigation of TGr cooperation by considering cooperation at the CBs level instead of the full TB. In this scenario, UE-T forwards only the successfully decoded CBs while applying the DF algorithm in case of SCS, along with associated signaling information indicating the indices of these CBs. The indexing overhead for CBs is minimal, as discussed in [14]. Meanwhile, UE-X applies SC at the CB level if SCS is configured.

In SSCS configuration, UE-T forwards both the decoded CBs and the soft bits of the CBs it fails to decode. In this configuration, it also forwards the two sets of index

information, one for the decoded CBs and another for the CBs whose soft bits are forwarded. And UE-X decides whether to apply SC or soft combining based on its own decoding status of each CB. If a CB is already decoded by UE-X, any corresponding data received from UE-T is discarded. If the CB is not decoded during the initial decoding attempt, UE-X applies SC if it receives the decoded CB from UE-T or performs soft combining if it receives the corresponding soft bits.

For this type of cooperation, we also incorporate CBG based HARQ retransmissions from the gNodeB. In this setup, HARQ retransmissions are CBG based. However, OLLA algorithm remains based on HARQ feedback at the TB level. To encourage higher MCS selection with this setup, we configure the target BLER to 30% (rather than the typical 10%) as highlighted in [29]. Despite this higher target, the actual BLER remains below the target value. The functionality of joint OLLA is unaffected, as it continues to operate on TB-level HARQ feedback. For joint HARQ per CBG the logic remains the same, except that both UEs would now provide HARQ feedback per CBG instead of per TB.

A. Limited CB based SSCS

We consider two limited CB-based SSCS schemes, previously proposed in our prior work in [14]. These schemes offer a trade-off between performance gains and the volume of data exchanged over the tethering link. Specifically, reducing the percentage of CBs shared for soft combining leads to reduced performance compared to sharing 100% of the CBs. In both schemes, if both UEs per TGr failed to decode the TB, soft combining is applied only on a subset of CBs corresponding to that TB. This subset is selected based on relatively lower SINR values among the CBs. The soft bits corresponding to these CBs can either be requested by UE-X or proactively forwarded by UE-T, depending upon the scheme. Any CBs that remain undecoded after soft combining are retransmitted by the gNodeB using CBG based HARQ.

- **CBs-UE-X:** In this scheme, UE-X identifies a limited percentage of CBs (based on their low SINR values) from the TB that it failed to decode and requests the corresponding soft bits from UE-T over the tethering link. UE-X sends the indexing information as specified in [14] and UE-T responds by sending only the requested soft bits.
- **CBs-UE-T:** In this scheme, UE-T proactively sends soft bits for a limited percentage of CBs from the TB, that it failed to decode, along with their indexing information [14]. UE-X then applies soft combining on these limited CBs if it was also unable to decode that CB initially.

V. Methodology for Performance Evaluation

We employ a dynamic system-level simulator (SLS), aligned with the methodology described in the SLS tutorial [30], to evaluate the proposed XR TGr framework.

TABLE II: PDCCH and PDSCH Decoding Status (Successfully Decoded: D and Fail to Decode: N/D) and Joint HARQ & OLLA for the Tethering Group with SCS and SSCS

| Scenario | UE-T | | | UE-X | | | SCS | | SSCS | | |
|----------|-------|-------|---------------|-------|-------|---------------|-------------|----------------------------------|---------------------|----------------------------------|---------------------|
| | PDCCH | PDSCH | HARQ Feedback | PDCCH | PDSCH | HARQ Feedback | | Joint HARQ gNodeB Retransmission | Enhanced Joint OLLA | Joint HARQ gNodeB Retransmission | Enhanced Joint OLLA |
| | | | | | | Initial | SoftC | | | | |
| 1 | D | D | ACK | D | D | ACK | - | | | | |
| 2 | D | D | ACK | D | N/D | NACK | - | | | | |
| 3 | D | D | ACK | N/D | N/D | - | - | | | | |
| 4 | D | N/D | NACK | D | D | ACK | - | | | | |
| 5 | D | N/D | NACK | D | N/D | NACK | ACK NACK | | | | |
| 6 | D | N/D | NACK | N/D | N/D | - | - | | | | |
| 7 | N/D | N/D | - | D | D | ACK | - | | | | |
| 8 | N/D | N/D | - | D | N/D | NACK | - | | | | |
| 9 | N/D | N/D | - | N/D | N/D | - | - | | | | |

The simulation setup adheres to the system model detailed in Section II, with parameters summarized in Table III. This simulator was also utilized in our previous study [15]. Calibration of the SLS is performed using the 3rd Generation Partnership Project (3GPP) new radio (NR) Release-18 XR evaluation guidelines as specified in [2].

The simulator simulates a comprehensive protocol stack, including application, transport, internet protocol, packet data convergence protocol, radio link control, medium access control, and physical layers. It supports key radio resource management (RRM) capabilities such as gNodeB scheduler, retransmission from the gNodeB based on HARQ feedback, CSI measurement and periodic reporting, and LA (both inner and outer loop), etc. Consistent with the 5G NR Time Division Duplex (TDD) structure, the simulator implements a slot-based transmission model using 14 orthogonal frequency-division multiplexing (OFDM) symbols per slot with a normal cyclic prefix [31]. We follow the DDDSU TDD frame structure in line with 3GPP NR XR evaluation criteria. It represents three DL slots, a special slot comprising of 10 DL symbols, two symbols as guard period and two symbols for uplink (UL) and lastly one complete UL slot.

For each TGr, the SINR is calculated for both UEs once DL PTM multicast transmission is scheduled depending upon the XR traffic for the UE-X of that TGr. The SINR calculations accounts for singular value decomposition (SVD) precoder at the transmitter, Multiple-Input and Multiple-Output (MIMO) configurations, channel effects, and the minimum mean square error-interference rejection combining (MMSE-IRC) receiver. The mean mutual information per bit (MMIB) is then derived for both UEs of the TGr utilizing their SINR [32]. The block error probability, which is obtained from the received SINR, MCS and MMIB via a precomputed look-up table produced from thorough link-level simulations, is used to determine the decoding success or failure for each UE of that TGr.

The gNodeB schedules transmissions in following order

- 1) HARQ retransmissions (if any for XR)
- 2) XR traffic
- 3) HARQ retransmissions (if any for eMBB)
- 4) eMBB traffic

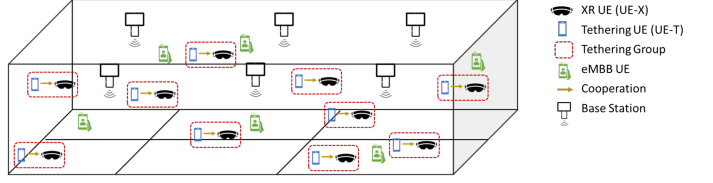


Fig. 2: Indoor hotspot scenario with XR TGrs.

The gNodeB schedules transmissions 3 and 4 only in scenarios where both traffic types coexists.

A. Deployment Scenario

This study evaluates the system performance under the following two standardized 3GPP defined deployment scenarios:

- 1) InH: This scenario models an indoor environment measuring 120×50 meters, with all users located indoors as shown in Fig. 2. The deployment includes 12 single-cell base stations, with 6 positioned in each of two parallel rows, separated by 20 meters of inter-site distance. The base stations are ceiling-mounted and operate at a lower transmit power relative to outdoor deployments.
- 2) DU: This scenario represents an outdoor dense urban environment spanning 528×60 meters, incorporating three-sector 7 base stations with a total of 21 cells as illustrated in Fig. 3. Buildings are randomly placed and it is assumed that 80% of the users are located indoors.

The channel characteristics for both deployment scenarios follow the 3GPP-defined models in [23].

B. Traffic Model

The specification in [2] is followed for generating the XR traffic. XR video frames of varying sizes are generated using truncated Gaussian distribution at a specified rate of 60 frames per second. The arrival of these frames at the gNodeB are modeled through a distinct truncated Gaussian distribution. $\mathcal{TN}(\mu, \sigma, a, b)$ is the notation for a truncated Gaussian distribution in Table III, where μ

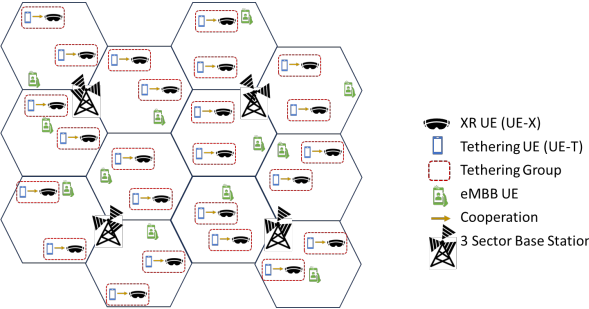


Fig. 3: Dense Urban scenario with XR TGrs.

and σ stand for the mean and standard deviation and a and b for the minimum and maximum bounds. 3GPP in [2] defined the key performance indicator (KPI), XR capacity, for measuring the capacity of the network with XR users, i.e., the maximum number of XR UEs that may be served per cell when at least 90% of them are happy. An XR user is considered happy if it successfully receive 99% of the frames (packets) within the packet delay budget (PDB).

For coexistence scenarios, we consider one eMBB user with full buffer traffic per cell in addition to the XR users. This indicates that there is unlimited data intended for the eMBB UE at the gNodeB waiting for scheduling and subsequent transmission.

For baseline simulations, only XR UEs are dropped in the network and the gNodeB transmits XR data via PTP (unicast) to each XR UE. These UEs have only single link to the network and are referred to as legacy XR UEs. Additionally, in case of coexistence scenario baseline simulations also include one eMBB UE per cell.

Each simulation runs for 9 seconds, enabling the evaluation of XR users satisfaction by verifying that 99% of packets are received within the PDB with a 99% confidence level and an error margin of 1.1%. The confidence level is calculated using the similar analogy as used in [22], i.e., 9 seconds simulation generates 540 packets per XR UE, which under the assumption of uncorrelated packets provides the required statistical confidence for the happiness metric. Simulations are repeated 10 times with different seeds to capture diverse user locations and channel conditions. For instance, with 7 XR UEs (or TGr) per cell, the system collect statistics from 840 XR UEs in InH scenario (7×10 drops \times 12 cells) and 1470 XR UEs in DU scenario (7×10 drops \times 21 cells). This approach facilitates estimation of XR capacity, with 7 XR UEs (or TGr) per cell, achieving 99% confidence level for an error margin of 2.6% for InH and for an error margin of 2% for DU scenario. The simulations are further repeated for varying numbers of XR UEs (or TGr) per cell, using uniformly distributed user locations and uniform load per cell.

VI. Simulation Results and Discussion

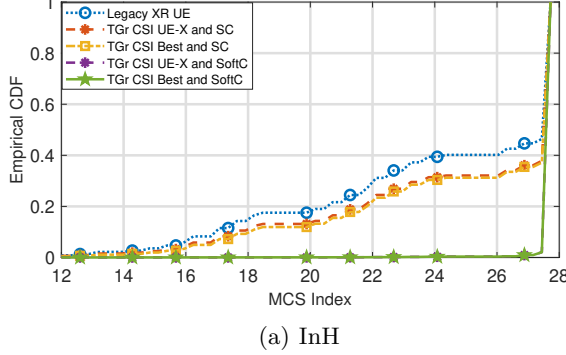
A. TB based Cooperation

TABLE III: Simulation Parameters

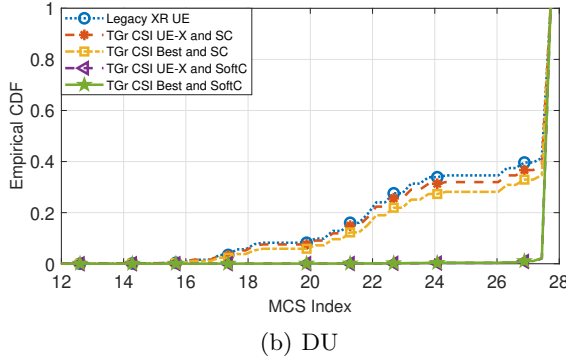
| Parameter Deployment | Setting | |
|------------------------------|---|--------------------|
| | InH | DU |
| Area | 120m \times 50m | 528m \times 460m |
| Layout | 12 cells | 21 cells |
| Inter-site Distance | 20m | 200m |
| gNodeB height | 3m | 25m |
| gNodeB power | 31 dBm | 51 dBm |
| Indoor UE Probability | 1 | 0.8 |
| Number of building floors | 1 | 6 |
| UE distribution among floors | uniform(1,6) | |
| Simulation Time | 9 seconds | |
| Simulation runs | 10 | |
| TTI length | 14 OFDM symbols | |
| TDD Frame Structure | DDDSU | |
| Bandwidth | 100 MHz | |
| Carrier Frequency | 4 GHz | |
| sub-carrier spacing | 30 kHz | |
| Modulation | QPSK to 256QAM | |
| XR frame rate | 60 fps | |
| XR random jitter | $\mathcal{TN}(0, 2, -4, 4)$ ms | |
| XR frame size (45 Mbps) | $\mathcal{TN}(93, 10, 46, 141)$ kB | |
| gNodeB antenna | 1 panel with 32 elements (4 \times 4 and 2 polarization) | |
| gNodeB Tx processing delay | 2.75 OFDM symbols | |
| UE height | 1.5m | |
| UE antenna | 4 omni-directional antennas (2 \times 1 and 2 polarization) | |
| UE receiver | MMSE-IRC | |
| UE speed | 3 km/h | |
| UE Rx processing delay | 6 OFDM symbols | |
| Scheduler | Proportional Fair | |
| CQI Measurement | Periodic every 2 ms | |
| CQI Reporting Delay | 2 ms | |
| Rank | 1 | |
| Channel Estimation | Ideal | |
| HARQ combining method | Chase soft combining | |
| Target BLER | 10% | |
| Intra TGr distance (x) | 1m | |

1) XR only: Initial simulations were conducted with only XR UEs / TGrs and the results are summarized in this subsection.

Figure 4 presents the MCS index selection as an empirical cumulative distribution function (eCDF). The results are presented for XR TGrs using both SC and SSCS, across two variations of CSI reporting per group (as discussed in Section II). For reference, the performance of legacy XR UEs is also shown. These results corresponds to scenarios with 7 XR users (legacy or TGr) per cell. The XR TGrs exhibit significantly improved MCS selection due to the proposed enhanced joint OLLA mechanism. Among the cooperation schemes, SSCS consistently delivers superior performance compared to SC. For instance, under the given simulation conditions, XR TGr with SSCS (for both CSI variations) select the highest available MCS index in approximately 98% of simulation time in both DU and InH scenarios. In contrast, XR TGrs with SC and CSI best select the highest MCS 65% of the time in DU and 63% in InH. The legacy XR UEs achieve this only 58% and 54% of the time in DU and InH, respectively. The impact of the two CSI reporting variations on SSCS performance with proposed enhanced joint OLLA algorithm is minimal across both deployment scenarios. However, the perfor-



(a) InH



(b) DU

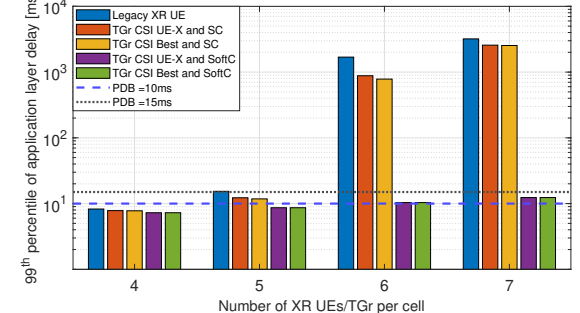
Fig. 4: MCS Index with 7 XR UEs per cell. (a) InH (b) DU.

TABLE IV: Propagation Status (PS) [%] of UEs within TGr with 7 XR TGrscell

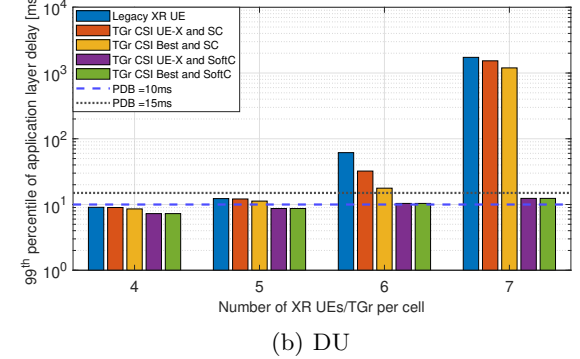
| Scenario | TGr PS | | DU | InH |
|----------|--------|------|------|------|
| | UE-X | UE-T | | |
| 1 | LOS | LOS | 48.3 | 98.8 |
| 2 | LOS | NLOS | 3.7 | 0 |
| 3 | NLOS | LOS | 6.8 | 1.2 |
| 4 | NLOS | NLOS | 41.2 | 0 |

formance difference due to CSI reporting variations is more visible for SCS in DU scenario compared to InH. This is attributed to greater SINR variability between the closely located UE-X and UE-T within a TGr in DU compared to InH. As shown in Table IV, the DU scenario exhibits a higher proportion of TGrs with UEs experiencing distinct propagation conditions (non-line-of-sight (NLOS) / line-of-sight (LOS)), contributing to greater SINR imbalance compared to InH. Nevertheless, under SSCS, performance remains consistent across CSI reporting variation.

Figure 5 illustrates the impact of TGr cooperation (SC and SSCS) with PTM transmission on application layer delay for varying numbers of XR UEs or TGrs per cell. The figure shows the 99th percentile of the eCDF of application layer delay. At lower user densities, both legacy XR UEs and XR TGrs experience similar delays. This is due to favorable SINR conditions and consequently, operation at maximum available MCS by both legacy XR UEs and XR



(a) InH

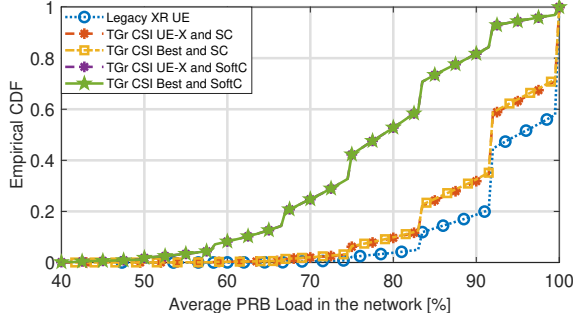


(b) DU

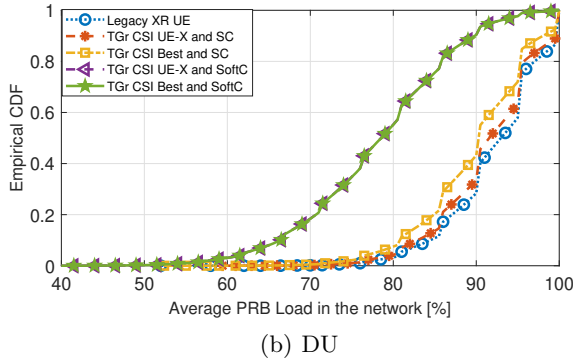
Fig. 5: 99th percentile of eCDF of application layer delay. (a) InH (b) DU.

TGr. TGrs offer no additional benefit because the MCS ceiling limits further gains. As user densities increases, network interference rises, degrading SINR and leading to lower MCS selection for legacy XR UEs. In contrast, TGrs employing SC or SSCS can sustain higher MCS values, thereby significantly reducing application layer delay, where SSCS offers higher gains. The interference impact is more severe in InH than in DU. For example, at 6 and 7 XR UEs per cell, legacy XR UEs in InH suffers considerably higher delay than in DU. However, XR TGr with SSCS maintain much lower delay in both deployments by operating at maximum MCS 98% of the time. This confirms the robustness of SSCS under high interference scenarios (or low-SINR conditions). TGr with SCS offer better performance than legacy XR UEs but fall short of the gains achieved by SSCS in lower SINR scenarios. The impact of CSI reporting variation on delay trends aligns with that observed in MCS index selection.

Figure 6 shows the average Physical Resource Block (PRB) utilization in the network when 7 XR UEs or TGrs are deployed per cell in both DU and InH scenarios. PTM multicast transmission with joint HARQ and enhanced joint OLLA to TGrs reduces PRB usage compared to the unicast transmission to legacy XR UEs. Specifically, TGr with SSCS utilize 14-16% fewer PRBs than legacy XR UEs at the 50th percentile, while TGr with SCS can save 1-3% PRBs. These gains stem from the ability of XR TGr to operate at higher MCS levels and lower BLERs (or fewer HARQ retransmissions) than legacy XR UEs



(a) InH



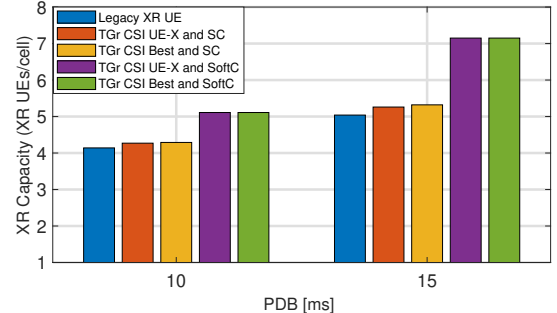
(b) DU

Fig. 6: Average PRB Load in the network with 7 XR UEs per cell. (a) InH (b) DU.

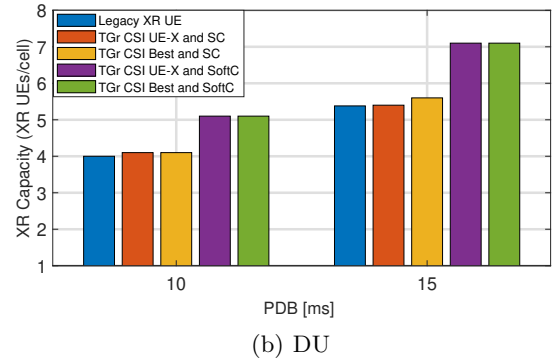
for given SINR. The extra PRBs can either support more XR user(s) or be allocated to other traffics in coexistence scenarios.

Figure 7 presents the XR capacity for XR TGr with SC and SSCS cooperation schemes alongside the baseline legacy XR UEs. The XR capacity is calculated with two PDB thresholds, i.e., 10ms and 15ms. The ability of XR TGr to operate at a higher MCS for a given SINR offers significant advantages over legacy XR UEs. Most notably, a substantial reduction in PRB utilization and application layer delay. These combined gains directly translate into a marked improvement in XR capacity, highlighting the benefits of the TGr-based cooperative approach under PTM transmission with joint HARQ and enhanced joint OLLA. XR TGr with SSCS outperforms both XR TGr with SC and legacy XR UE. For instant, TGr with SSCS offer XR capacity improvements of 23-27% (PDB = 10ms) and 32-42% (PDB = 15ms) over legacy XR UEs in both deployment scenarios. In contrast, TGr with SCS show modest capacity gains of 2.5-4% under both PDB targets. The two variations of CSI per TGr resulted in smaller performance difference with SSCS cooperation scheme compared to SCS. Furthermore, the performance difference of XR TGr with SCS for two CSI variations is less pronounced in InH scenario compared to DU.

2) XR UEs plus one eMBB UE: In the coexistence scenario, one eMBB UE with full buffer traffic per cell is added alongside the existing XR UEs / TGrs per cell. This setup enhances interference to XR users, under



(a) InH



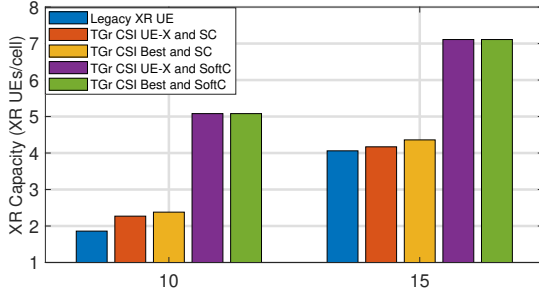
(b) DU

Fig. 7: XR Capacity (XR users only) vs PDB. (a) InH (b) DU.

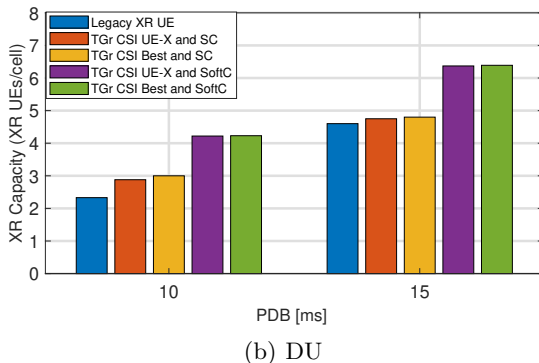
the scheduling constraint that XR traffic is prioritized, followed by eMBB traffic.

Figure 8 illustrates the XR capacity of the network for two PDB values (10ms and 15ms). As expected, the XR capacity of the network drops compared to XR-only scenario (network with XR UEs / TGrs). The addition of a eMBB UE with full buffer traffic per cell increases the interference in the system, which ultimately reduces XR capacity. However, the relative performance gains of XR TGrs are higher than in the XR-only case. Specifically, in the InH scenario, XR TGr achieve gains of 3-28% with SCS and 75-173% with SSCS, while in DU the gains are 3-29% with SCS and 38-82% with SSCS. Notably, in InH, the performance of XR TGr with SSCS remains largely unaffected by the added eMBB interference, maintaining nearly the same performance as in the XR-only case and outperforming legacy XR UEs by a greater margin.

XR TGr not only provide performance gains for XR UEs by increasing the XR capacity but it also contribute to better eMBB performance in the coexistence scenarios. XR TGr especially with SSCS require fewer PRBs for XR traffic, leaving more resources available for eMBB traffic. Figure 9 presents the eCDF of average eMBB throughput for the cases when there is one eMBB UE with 4 legacy XR UEs and one eMBB UE with 4 XR TGrs per cell. The results show that XR TGr with SSCS achieve higher average eMBB throughput than legacy XR UEs in both InH and DU. This improvement is primarily due to the reduced PRBs utilization of XR TGrs



(a) InH



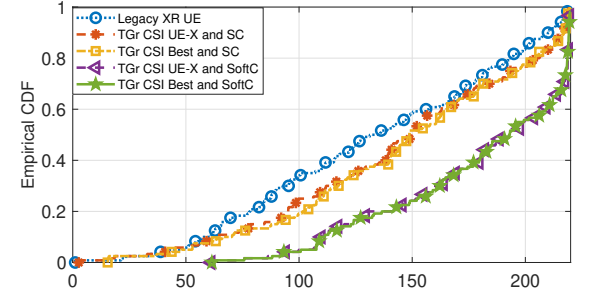
(b) DU

Fig. 8: XR Capacity (XR users plus 1eMBB user) vs PDB. (a) InH (b) DU.

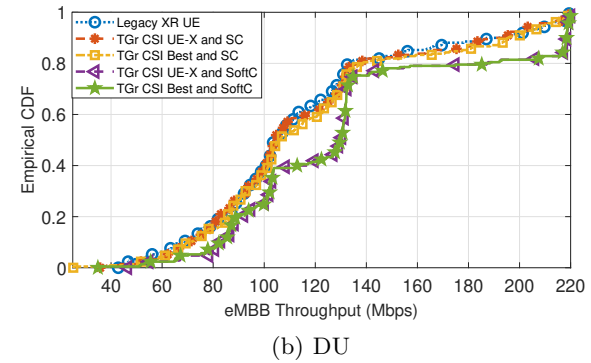
compared to legacy XR UEs for approximately similar amount of transmitted data. The gains of XR TGr with SCS are smaller particularly in DU, where they are almost negligible. Quantitatively, XR TGr with SSCS achieves a 43% throughput gain for eMBB at the 50th percentile in InH and of 25% in DU compared to legacy XR UEs, whereas XR TGr with SCS provide only 10% and 1% gain in InH and DU, respectively.

B. CB based Cooperation

This subsection summarizes the findings from the CB-based cooperation analysis, which was conducted exclusively for the InH deployment scenario. Figure 10 presents the XR capacity of the InH scenario for legacy XR UEs and XR TGr under both cooperation schemes, considering a network with XR UEs only. The use of CBG based HARQ retransmissions and higher target BLER improve the performance of legacy XR UEs and XR TGr with SCS marginally compared to TB based cooperation and HARQ retransmission cases of legacy XR UEs and XR TGr with SCS, respectively. However, the performance of TGr with SSCS remains nearly the same as in the TB based cooperation case. This is because SSCS operate at maximum available MCS most of the time with a lower BLER under the given conditions, resulting in very few HARQ retransmissions, so changing the granularity of HARQ retransmission does not affect its performance. Nevertheless, SSCS still delivers substantial gains, ranging from 22-35% over legacy XR UEs.



(a) InH



(b) DU

Fig. 9: eMBB Throughput with 4 XR UEs/TGr per cell. (a) InH (b) DU.

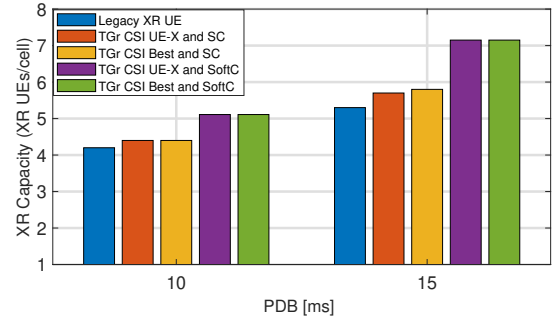


Fig. 10: XR Capacity with CB based HARQ and cooperation in InH with XR UEs only.

Figure 11 compares the XR capacity for XR TGr using limited CB-based SSCS with legacy XR UEs and TGr with SSCS using 100% CB in the InH scenario. The results indicate that limited CB-based cooperation achieve XR capacity gains that lie between XR capacity achievable through legacy XR UEs and XR TGr with SSCS using 100% CBs. The two variations of limited CB-based SSCS exhibit almost identical average performance. Importantly, limited CB-based cooperation offers a practical trade-off between the amount of data exchanged over the tethering link and the performance gains achieved by the TGr. In the extreme case where no data is exchanged over the tethering link, the TGr's performance matches that of legacy XR UEs.

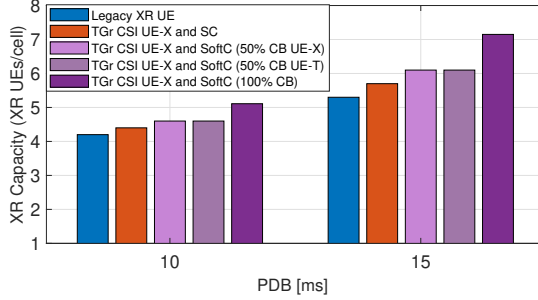


Fig. 11: XR Capacity with 50% CB in InH with XR UEs only.

C. Discussion

The XR TGr with SSCS substantially improves network XR capacity compared to legacy XR UEs (single link connected devices) in both InH and DU scenarios. By enabling XR devices to operate at a higher MCS while maintaining a post-cooperation BLER equal to or less than the target BLER, XR TGr not only reduces application-layer delay but also frees up network resources (fewer PRBs utilization). These additional resources can be utilized to accommodate more XR devices or to support more eMBB traffic in coexistence scenarios.

The performance gains of XR TGr in terms of XR capacity are nearly identical and in some cases almost equivalent, whether both UEs in the TGr provide CSI feedback or only one UE per TGr does. This observation enables the possibility of configuring only one UE per TGr for CSI reporting, thereby reducing the UL resources for CSI to the same level as in legacy XR UEs. The only additional UL resources used by TGr, compared to legacy XR UE, for optimizing DL transmissions are those required for HARQ feedbacks from the tethering UE and from the XR UE in SSCS after soft combining.

It is important to note that this study assumes an ideal tethering link; hence, reported network capacity improvements be regarded as upper-bound values. In practice, the tethering link's performance will influence the realized gains and this performance will depend on the specific technology used for tethering. For example, a tethering link operating on an independent carrier frequency than cellular network's one may introduce no additional interference to the direct link (gNodeB-UE). However, latency on the tethering link could degrade TGr performance in certain cases. For instance, when a TB fails on XR device initial decoding (before any cooperation) and is already near the end of its PDB. In such situations, if the tethering UE provides the correct TB (or soft bit corresponding to that TB) shortly afterward, the additional delay could cause a PDB violation. However, in such situations even HARQ retransmission are insufficient. Cooperation over the tethering link may be more effective than HARQ retransmissions when the failed TB has a margin of only a few milliseconds before PDB expiry. This is because the tethering link is expected to have lower

latency than HARQ retransmission from the gNodeB for two key reasons, i.e., the short physical distance between the two UEs in the TGr and the absence of scheduling delays on the tethering link, as it could be dedicated. In contrast, HARQ retransmissions from the gNodeB usually involve longer distances and small but non-negligible, scheduling delays, which depend on the TDD frame structure.

1) Complexity and Overhead Analysis of TGr: In this section, we discuss the complexity introduced by the TGr for both gNodeB and UEs along with the signaling overhead.

- **gNodeB Computational Complexity:** When XR TGrs are enabled, the gNodeB must collect HARQ feedback from both member UEs, take a retransmission decision based on joint HARQ feedback processing and apply the enhanced joint OLLA algorithm. These additional steps add only a negligible constant offset in gNodeB complexity. Consequently, the additional control-plane work is a small constant per TGr and does not change the asymptotic scaling, i.e., the gNodeB processing remains $\mathcal{O}(N)$ for N users, with only a modest constant increase.
- **UE Computational Complexity:** In the legacy XR UEs case, XR UE performs standard demodulation/decoding procedure and return HARQ feedback. In the XR TGr case, both UE-T and UE-X run the standard decoding chain and provide HARQ feedback plus some additional steps depending upon the cooperation scheme.
 - **SCS:** UE-T runs DF algorithm and forwards decoded TB when successfully decoded. UE-X performs SC (i.e., it uses the first successful copy of the TB). These additions impose only negligible extra arithmetic processing beyond the baseline decode operations.
 - **SSCS:** If UE-T failed to decode the PDSCH but successfully decoded the PDCCH then it will forward the soft bits (LLRs). UE-X then optionally performs element wise soft combining of the soft bits (LLRs) (an $\mathcal{O}(L)$ operation for a TB with L LLR entries) followed by a secondary decode and HARQ feedback. Thus SSCS introduces additional per TB arithmetic processing step that scales with TB size.

From an energy perspective, XR TGr operation can be substantially more demanding than legacy XR UEs because two UEs may be decoding and one may be forwarding data. The total per TGr energy exceeds the combined energy of two legacy XR UEs (due to forwarding of the data and selection or soft combining).

- **Signaling Overhead:** A legacy XR UEs provide one HARQ feedback per TB (usually one bit if HARQ feedback is per TB) for the initial transmission and one CSI report (periodic or aperiodic). For XR TGr:
 - **SCS:** two HARQ feedback per TB for the initial

transmission.

- SSCS: two initial HARQ feedback per TB plus a conditional secondary HARQ feedback from UE-X only when soft combining is performed.

To limit resources utilized for CSI, the XR TGr could be configured such that only one UE per TGr report CSI with negligible performance degradation in many scenarios, so resources utilized for CSI would be similar for both legacy XR UEs and XR TGrs. Since HARQ feedback is extremely small often just one bit for TB based HARQ retransmissions, so the signaling overhead (UL resource cost) of enabling these DL gains is very small. Moreover, in lower user densities, the cooperation gain of the XR TGr cannot choose higher MCS than the legacy XR UEs (maximum MCS is capped and legacy XR UEs are already operating at maximum MCS) but this cooperation reduces the number of retransmissions from the gNodeB which tends to lower overall gNodeB scheduling and physical layer load for the given user.

Enabling XR TGr requires only small changes to the standard, slight modifications in gNodeB control logic with small constant overhead and introduces modest additional UE computation. Taken together, the complexities and overheads are small compared with the substantial gains in spectral efficiency that this cooperative framework delivers especially for the time-bound XR application.

VII. Conclusion

This paper presented an approach for optimizing PTM transmission to multi-connected XR TGr with the objective of enhancing network XR capacity. An enhanced joint OLLA algorithm was proposed to exploit the benefits of either SCS or SSCS cooperation scheme in the LA process for PTM transmission. The method leverages HARQ feedback from both UEs in an XR TGr to optimize the MCS based on the post-cooperation BLER of the UE-X. Coupled with a joint HARQ feedback processing algorithm, the proposed enhanced joint OLLA enables the network to operate at higher spectral efficiency, thereby reducing PRB usage per XR user and lowering application layer delay. The delay reduction and lower PRB utilization increases the likelihood of meeting the XR "happiness" criteria for more users, while extra PRBs can also be utilized to support more eMBB traffic, ultimately boosting overall network capacity. The algorithm also demonstrates robustness in MCS optimization, achieving near identical performance even when only one UE per TGr is configured to provide CSI, thus reducing the UL resource overhead for XR TGr operation under the given channel conditions.

Dynamic system level simulations show that XR TGrs with joint HARQ feedback processing and enhanced joint OLLA achieve XR capacity gains in the range of 23-42% with SSCS cooperation in XR-only scenarios. These gains become even more pronounced under higher-interference coexistence scenarios involving XR and eMBB users, where SSCS cooperation yields improvements in the range

of 38-173%. Furthermore, in coexistence scenarios with four XR users and one eMBB user, eMBB throughput increases by 25-43% due to lower PRB utilization by XR TGrs.

Abbreviations

| | |
|----------|--|
| 3GPP | 3rd Generation Partnership Project |
| 5G-A | 5th generation-advanced |
| ACK | Acknowledgment |
| AR | Augmented reality |
| BLER | block error rate |
| CB | Code block |
| CBG | Code block group |
| CC | Chase combining |
| CSI | Channel state information |
| CQI | Channel quality indicator |
| DU | Dense urban |
| DL | Downlink |
| DF | Decode-and-forward |
| eMBB | Enhanced mobile broadband |
| eCDF | Empirical cumulative distribution function |
| gNodeB | Next-generation node B |
| HARQ | Hybrid automatic repeat request |
| ILLA | Inner loop link adaptation |
| InH | Indoor hotspot |
| ICI | Inter-cell interference |
| LA | Link adaptation |
| LOS | Line-of-sight |
| LLR | Log-likelihood ratio |
| MMIB | Mean mutual information per bit |
| mmWave | Millimeter-wave |
| MIMO | Multiple-Input and Multiple-Output |
| MBS | Multicast and broadcast services |
| MMSE-IRC | Minimum mean square error-interference rejection combining |
| MCS | Modulation and coding scheme |
| MR | Mixed reality |
| NR | New radio |
| NACK | Negative acknowledgment |
| NLOS | Non-line-of-sight |
| OFDM | Orthogonal frequency-division multiplexing |
| OLLA | Outer loop link adaptation |
| PDB | Packet delay budget |
| PTM | Point-to-multipoint |
| PTP | Point-to-point |
| PRB | Physical resource block |
| PDSCH | Physical downlink shared channel |
| PDCCH | Physical downlink control channel |
| QoS | Quality of service |
| RRM | Radio resource management |
| Rx | Receive |
| SC | Selection combining |
| SCS | Selection combining Scheme |
| SSCS | Selection/Soft combining scheme |
| SVD | Singular value decomposition |
| soft-DF | Soft decode-and-forward |
| SINR | Signal-to-interference-plus-noise ratio |
| SLS | System-level simulator |

| | |
|-------|---|
| TBLER | Transport block error rate |
| TGr | Tethering group |
| TB | Transport block |
| Tx | Transmit |
| TDD | Time division duplex |
| UE | User equipment |
| UE-X | User equipment-extended reality |
| UE-T | User equipment with tethering |
| UL | Uplink |
| URLLC | Ultra reliable low latency communications |
| VR | Virtual reality |
| WLAN | Wireless local-area network |
| XR | Extended reality |

References

- [1] G. Minopoulos and K. E. Psannis, "Opportunities and Challenges of Tangible XR Applications for 5G Networks and Beyond," in IEEE Consumer Electronics Magazine, vol. 12, no. 6, pp. 9-19, 1 Nov. 2023.
- [2] 3GPP TR 38.838 V17.0.0, "Technical Specification Group Radio Access Network; Study on Extended Reality (XR) Evaluations for NR (Release 17)," Tech. Rep., December 2021.
- [3] P. Paymard, A. Amiri, T. E. Kolding and K. I. Pedersen, "Enhanced CQI to Boost the Performance of 5G-Advanced XR With Code Block Group Transmissions," in IEEE Transactions on Vehicular Technology, vol. 73, no. 4, pp. 4774-4786, April 2024.
- [4] P. Paymard, S. Paris, A. Amiri, T. E. Kolding, F. S. Moya and K. I. Pedersen, "PDU-set Scheduling Algorithm for XR Traffic in Multi-Service 5G-Advanced Networks," ICC 2024 - IEEE International Conference on Communications, Denver, CO, USA, 2024, pp. 758-763.
- [5] M. Gapeyenko, V. Petrov, S. Paris, A. Marcano and K. I. Pedersen, "Standardization of Extended Reality (XR) over 5G and 5G-Advanced 3GPP New Radio," in IEEE Network, vol. 37, no. 4, pp. 22-28, July/August 2021.
- [6] M. Gapeyenko et al., "Overview of NR Enhancements for Extended Reality (XR) in 3GPP 5G-Advanced," in IEEE Access, vol. 12, pp. 186941-186956, 2024.
- [7] F. Hu, Y. Deng, W. Saad, M. Bennis and A. H. Aghvami, "Cellular-Connected Wireless Virtual Reality: Requirements, Challenges, and Solutions," IEEE Communications Magazine, vol. 58, pp. 105-111, 2020.
- [8] M. A. Javed, P. Liu and S. S. Panwar, "Enhancing XR Application Performance in Multi-Connectivity Enabled mmWave Networks," in IEEE Open Journal of the Communications Society, vol. 4, pp. 2421-2438, 2023.
- [9] Z. Gu, H. Lu, P. Hong and Y. Zhang, "Reliability Enhancement for VR Delivery in Mobile-Edge Empowered Dual-Connectivity Sub-6 GHz and mmWave HetNets," in IEEE Transactions on Wireless Communications, vol. 21, no. 4, pp. 2210-2226, April 2022.
- [10] M. Susloparov, A. Krasilov and E. Khorov, "Boosting XR Capacity With Multi-Band Multi-Connectivity in 5G Systems," in IEEE Communications Letters, vol. 28, no. 9, pp. 2211-2215, Sept. 2024.
- [11] N. H. Mahmood, A. Karimi, G. Berardinelli, K. I. Pedersen and D. Laselva, "On the Resource Utilization of Multi-Connectivity Transmission for URLLC Services in 5G New Radio," 2019 IEEE Wireless Communications and Networking Conference Workshop (WCNCW), Marrakech, Morocco, pp. 1-6, 2019.
- [12] E. J. Khatib, D. A. Wassie, G. Berardinelli, I. Rodriguez and P. Mogensen, "Multi-Connectivity for Ultra-Reliable Communication in Industrial Scenarios," 2019 IEEE 89th Vehicular Technology Conference (VTC2019-Spring), Kuala Lumpur, Malaysia, pp. 1-6, 2019.
- [13] M. Ahsen, B. Yanakiev, C. Rosa, C. N. Manchon and R. Adeogun, "Cooperative Multicast for Multi-Connected XR Devices with Joint HARQ Processing," 2024 IEEE 35th International Symposium on Personal, Indoor and Mobile Radio Communications (PIMRC), Valencia, Spain, 2024, pp. 1-6.
- [14] M. Ahsen, B. Yanakiev, C. Rosa and R. Adeogun, "Enhancing Multi-Connected XR Device Performance With Soft Combining and Joint HARQ Processing in Cooperative Multicast," in IEEE Open Journal of the Communications Society, vol. 6, pp. 2438-2452, 2025.
- [15] M. Ahsen, B. Yanakiev, C. Rosa and R. Adeogun, "Boosting XR Capacity Through Multi-Connected XR Tethering Groups With Selection Combining," 2025 IEEE International Symposium on Personal, Indoor and Mobile Radio Communications (PIMRC), 2025.
- [16] 3GPP TR 26.806 V18.0.0, "Study on Tethering AR Glasses – Architectures, QoS and Media Aspects (Release 18)," Tech. Rep., June 2023.
- [17] E. W. Jang, J. Lee, H. -L. Lou and J. M. Cioffi, "On the combining schemes for MIMO systems with hybrid ARQ," in IEEE Transactions on Wireless Communications, vol. 8, no. 2, pp. 836-842, Feb. 2009.
- [18] S. Park and S. Choi, "Performance of Symbol-Level Combining and Bit-Level Combining in MIMO Multiple ARQ Systems," in IEEE Transactions on Communications, vol. 64, no. 4, pp. 1517-1528, April 2016.
- [19] G. Pocovi, A. A. Esswie, and K. I. Pedersen, "Channel quality feedback enhancements for accurate URLLC link adaptation in 5G systems," in 2020 IEEE 91st Veh. Technol. Conf. (VTC2020-Spring), May, 2020.
- [20] A. Duran et al., "Self-optimization algorithm for outer loop link adaptation in LTE," IEEE Commun. Lett., vol. 19, no. 11, pp. 2005-2008, Sep., 2015.
- [21] P. Paymard, A. Amiri, T. E. Kolding and K. I. Pedersen, "Performance of Joint XR and Best-Effort eMBB Traffic in 5G-Advanced Networks," 2023 IEEE 97th Vehicular Technology Conference (VTC2023-Spring), Florence, Italy, 2023, pp. 1-5.
- [22] P. Paymard, A. Amiri, T. E. Kolding and K. I. Pedersen, "Optimizing Mixed Capacity of Extended Reality and Mobile Broadband Services in 5G-Advanced Networks," in IEEE Access, vol. 11, pp. 113324-113338, 2023.
- [23] 3GPP TR 38.901 V17.0.0, "Study on channel model for frequencies from 0.5 to 100 GHz (Release 17)," Tech. Rep., March 2022.
- [24] V. K. Shrivastava, S. Baek and Y. Baek, "5G Evolution for Multicast and Broadcast Services in 3GPP Release 17," in IEEE Communications Standards Magazine, vol. 6, no. 3, pp. 70-76, September 2022.
- [25] J. N. Laneman, D. N. C. Tse and G. W. Wornell, "Cooperative diversity in wireless networks: Efficient protocols and outage behavior," in IEEE Transactions on Information Theory, vol. 50, no. 12, pp. 3062-3080, Dec. 2004.
- [26] H. S. Sneessens and L. Vandendorpe, "Soft decode and forward improves cooperative communications," in Proc. IEEE Int. Workshop Computational Advances Multi-Sensor Adaptive Processing, Puerto Vallarta, Mexico, Dec. 2005, pp. 157-160.
- [27] J. Hagenauer, E. Offer, and L. Papke, "Iterative decoding of binary block and convolutional codes," IEEE Trans. Inf. Theory, vol. 42, pp. 429-445, Mar. 1996.
- [28] 3GPP TS 38.213 V18.0.0, "NR; Physical layer procedures for control (Release 18)," Tech. Spec., September 2023.
- [29] P. Paymard, A. Amiri, T. E. Kolding and K. I. Pedersen, "Enhanced Link Adaptation for Extended Reality Code Block Group based HARQ Transmissions," 2022 IEEE Globecom Workshops (GC Wkshps), Rio de Janeiro, Brazil, 2022, pp. 711-716.
- [30] K. Pedersen, R. Maldonado, G. Pocovi, E. Juan, M. Lauridsen, I. Z. Kovács, et al., "A tutorial on radio system-level simulations with emphasis on 3GPP 5G-advanced and beyond", IEEE Commun. Surveys Tuts., Mar. 2024.
- [31] 3GPP TS 38.211 V18.0.0, "NR; Physical channels and modulation (Release 18)," Tech. Spec., September 2023.
- [32] T. Tang, R. Doostnejad and T. J. Lim, "Mean mutual information per coded bit based precoding in MIMO-OFDM systems", Proc. IEEE 72nd Veh. Technol. Conf., pp. 1-5, Sep. 2010.



MUHAMMAD AHSEN (Graduate Student Member, IEEE) received the B.E. degree in Electrical Engineering in 2013 and the M.S. degree(Hons.) in Electrical Engineering in 2016 from the National University of Sciences and Technology (NUST), Islamabad, Pakistan. He is currently pursuing the Ph.D. degree with the Department of Electronics Systems, Aalborg University, Denmark, in collaboration with Nokia Standard, Aalborg, Denmark. His research interest includes extended reality communications, 5G/6G radio resource management, cooperative communication and time-sensitive wireless communication.

extended reality communications, 5G/6G radio resource management, cooperative communication and time-sensitive wireless communication.



BOYAN YANAKIEV received the B.Sc. degree in physics from Sofia University, Bulgaria, in 2006, and the M.Sc. and Ph.D. degrees from Aalborg University, Aalborg, Denmark, in 2008 and 2011, respectively. He is currently with Nokia Standardization Research, Denmark, focusing on 5G advanced and 6G topics. His current work is in the area of XR optimization in RAN



CLAUDIO ROSA received his M.Sc. E.E. and Ph.D. degrees in 2000 and 2005, respectively, from Aalborg University. In 2003 he also received an M.Sc.E.E. degree in telecommunication engineering from Politecnico di Milano, Italy. Since he joined Nokia in 2005, he contributed to standardization of 4G and 5G systems working on uplink power control and radio resource management, carrier aggregation, dual connectivity, and unlicensed spectrum operation. His current research interests also include user plane protocol design for 6G, flexible duplexing and radio enablers for eXtended reality applications. He has filed more than 200 patent applications, holds more than 50 granted patents, and has co-authored more than 50 scientific publications.



RAMONI ADEOGUN (Senior Member, IEEE) received the B.Eng. degree in electrical and computer engineering from the Federal University of Technology, Minna, Nigeria, and the Ph.D. degree in electronic and computer systems engineering from the Victoria University of Wellington, New Zealand in 2007 and 2015, respectively. He is currently an Associate Professor and leader of the AI for Communications group at Aalborg University, Denmark. Prior to joining Aalborg University, he held various academic and industry research positions at University of Cape Town, South Africa, Odua Telecoms Ltd., and the National Space Research and Development Agency, Nigeria. His research interests include signal processing, machine learning and AI for PHY MAC and RRM. He has co-authored over 70 peer-reviewed publications.